Heliyon 9 (2023) e15028

Contents lists available at ScienceDirect

Heliyon

journal homepage: www.cell.com/heliyon

Review article

Atmospheric deterioration of ceramic building materials and future trends in the field: a review

Ana C. Santa [a], Maryory A. Gómez [b], Juan G. Castaño [b], José A. Tamayo [a], Libia M. Baena [c,*]

[a] Grupo Calidad Metrología y Producción, Instituto Tecnológico Metropolitano –ITM, Medellín, Antioquia, 050034, Colombia
[b] Centro de Investigación, Innovación y Desarrollo de Materiales – CIDEMAT, Facultad de Ingeniería, Universidad de Antioquia UdeA, Calle 70 No 52 – 21, Medellín, Colombia
[c] Grupo de Química Básica, Aplicada y Ambiente (Alquimia), Instituto Tecnológico Metropolitano (ITM), Medellín, Colombia

ARTICLE INFO

Keywords:
Atmospheric deterioration
Ceramic building materials
Concrete
Atmospheric pollutants
Content

ABSTRACT

Multiple techniques have been developed and implemented around the world to monitor structures and minimize the costs of repairing, maintaining, and losing ceramic building materials due to environmental factors. Understanding the different degradation phenomena that affect ceramic building materials and evaluating their condition can help reduce material losses caused by deterioration and the need for interventions. This study reviews the main forms of atmospheric degradation that affect ceramic materials and the commonly employed methods to evaluate their deterioration. The aim is to illustrate the different types of atmospheric deterioration that affect ceramic materials and to demonstrate the current monitoring methods and testing. In addition to a literature review, a bibliometric analysis was conducted to highlight the available tools to counter atmospheric deterioration. The analysis shows that CO2, sulfates, and temperature are the most important types of degradation for ceramic construction materials. It was also discovered that due to their porous nature, ceramic construction materials require careful control as contaminants and water can easily penetrate them. The two most severe types of deterioration identified in this analysis for reinforced concrete were chloride-induced corrosion and carbonation.

1. Introduction

Pollution and climate change have had a significant impact on the ceramic materials used in construction [1]. Temperature can cause freezing, thawing, and thermal shock, all of which can affect materials in different ways. Water can affect materials through precipitation, moisture cycles, and moisture time. Air can have various impacts, including rain, wind, sand, and salt. Finally, pollution can impact materials through sulfur dioxide, nitrogen dioxide, carbon dioxide, pH, and other factors. It is important to consider these factors when working with materials to ensure their longevity and durability. By understanding how these factors can affect materials, it is possible to take steps to protect them from damage or deterioration [2].

Without a question, cement is the building material that is utilized the most frequently worldwide. However, it costs many trillions of euros every year to maintain, fix, and rejuvenate this material. This investment accounts for 4% of the GDP of wealthy nations, and

* Corresponding authorInstituto Tecnológico Metropolitano –ITM, Medellín, Antioquia, Colombia.
E-mail address: anasanta304720@correo.itm.edu.co (L.M. Baena).

https://doi.org/10.1016/j.heliyon.2023.e15028
Received 14 October 2022; Received in revised form 23 March 2023; Accepted 24 March 2023
Available online 30 March 2023
2405-8440/© 2023 The Authors. Published by Elsevier Ltd. This is an open access article under the CC BY-NC-ND license (http://creativecommons.org/licenses/by-nc-nd/4.0/).

in certain cases considerably more [3,4].

Over time, exposure to atmospheric conditions can cause significant damage to ceramic building materials. This damage often requires expensive repairs, and in rare cases, may even compromise the stability of specific structural components [5]. Climate change has altered the conditions under which concrete operates, leading to an acceleration in its degradation process. The corrosion of steel bars within structures can cause reinforced concrete to crack and spall [6].

Bricks, another commonly used ceramic material in construction, are typically resistant to atmospheric agents such as acid rain. However, accumulation and crystallization of salts, especially sulfate ions, in their pores can cause rapid atmospheric deterioration. Additionally, the mortar used in construction, which contains calcium oxide, can be easily dissolved by rainwater, leading to the loss of sand grains. Limestone and marble are also susceptible to deterioration due to water condensing in their fissures and expanding when frozen, causing the material to crack [7].

The degradation of ceramic materials due to atmospheric action is a topic of ongoing research, given the significant economic losses it causes to facades, buildings, and cultural artifacts. This review article serves to highlight the various ways in which these materials can deteriorate under the influence of atmospheric variables, and to showcase the most actively researched areas in this field. Special attention is given to illustrating the various tests that can be performed on these materials to prevent deterioration, providing researchers with practical tools for writing essays on the subject.

This literature review covers several aspects related to the atmospheric degradation of ceramic building materials. Firstly, it outlines the primary forms of degradation that can occur due to atmospheric action. Secondly, it provides an overview of commonly used tests and characterization techniques that can help quantify, analyze, and prevent deterioration in popular ceramic building materials. Thirdly, it includes a bibliometric analysis that highlights various tools available for mitigating atmospheric deterioration of ceramic building materials. It's worth noting that, to the best of our knowledge, this is the first bibliometric analysis conducted on the topic of atmospheric degradation of ceramic building materials.

2. Methodology

The use of Scopus® was critical to this study as it served as the primary source of information. Scopus® is a comprehensive database that contains recent scientific information, enabling easy access and bibliometric analysis of published literature across a wide range of subjects and sources. Through the information gathered from Scopus®, a bibliometric analysis was conducted, and maps were generated to understand global trends regarding the degradation of ceramic building materials, specifically concretes. The analysis allowed for the identification of the various types of degradation of these materials and the primary atmospheric agents responsible for their deterioration. Finally, the study identified the main trends in the construction of atmospheric degradation maps for ceramic building materials. This review utilized data obtained from Scopus® on February 1, 2022, and was focused on documents published between 1985 and 2022 that addressed atmospheric degradation maps for commonly used ceramic materials. To perform the bibliometric analysis, three search equations (referred to as Q1, Q1-A, and Q1-B) were defined and applied to the title, abstract, and keyword fields of English language documents. Fig. 1 provides a detailed overview of the results obtained from each search.

3. Bibliometric analysis and bibliometric networks

The search equation Q1 (as shown in Table 1) was used to find the most widely studied ceramic materials used in construction. Fig. 1 shows the number of documents retrieved by each of the three search equations (Q1, Q1-A, and Q1-B). Q1 retrieved a notably high number of documents because it included all terms related to the ceramic materials of greatest interest in the construction sector. Q1-A, which added terms related to deterioration and degradation, also retrieved a high number of publications. Finally, Q1-B (using the terms listed in Table 1) retrieved 184 documents.

The bibliometric analysis presented below was conducted using the group of publications retrieved by Q1-B. Fig. 2 illustrates the global distribution of the publications retrieved by Q1-B, showing that the United States and Canada have the highest number of publications on the topic. Moreover, the study observed a clear trend where 21 countries have only one publication on the topic. Thirteen of the retrieved documents did not specify a particular country.

Fig. 3 presents the document types retrieved by Q1-B. Most of them are research articles (53%) and conference proceedings (37%). Review papers (4%), conference reviews (3%), book chapters (2%), and books (1%) address this topic to a lesser extent.

Fig. 4 is the network of keywords found with Q1-B with co-occurrence of three, that is, terms that are found at least three times in the publications retrieved by Q1-B. full counting method was used to include all the keywords in the documents regardless of the number of times they appeared in each publication" instead of "a thesaurus was created to compile the terms that had the same meaning in this study.

In Fig. 4, the biggest circles represent the most common keywords in the documents, e.g., *reinforced concrete* and *corrosion* in yellow; *building materials* and *degradation* in red; *non-destructive test* in purple; and *penetrating radar* in blue. This means that the 184 documents

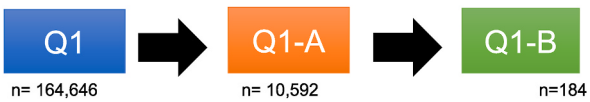

Fig. 1. Number of articles retrieved by three search equations.

Table 1
Search equations (Q) used in his study to find documents about degradation in building materials.

Q1	Q1-A	Q1-B
("Building materials" OR "History masonry" OR "Reinforced concrete" OR "Red clay brick" OR " Portland building cement" OR "mansory materials" OR "Historical heritage" OR "Building concrete")	(Q1) AND ("degradation" OR "deterioration")	Q1-A AND ("Maps" OR "atmospheric corrosion maps" OR "mapping" OR "deterioration maps" OR "degradation maps"))

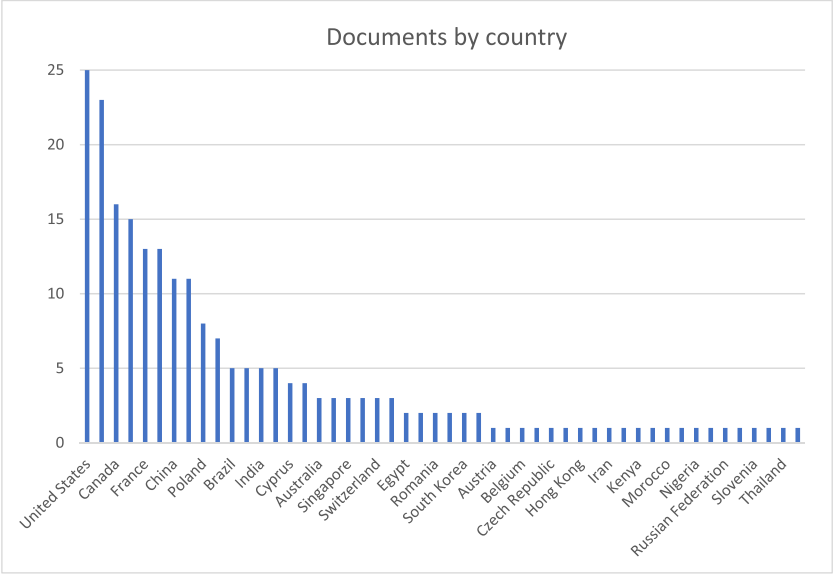

Fig. 2. Global distribution of the publications retrieved by equation Q1-B.

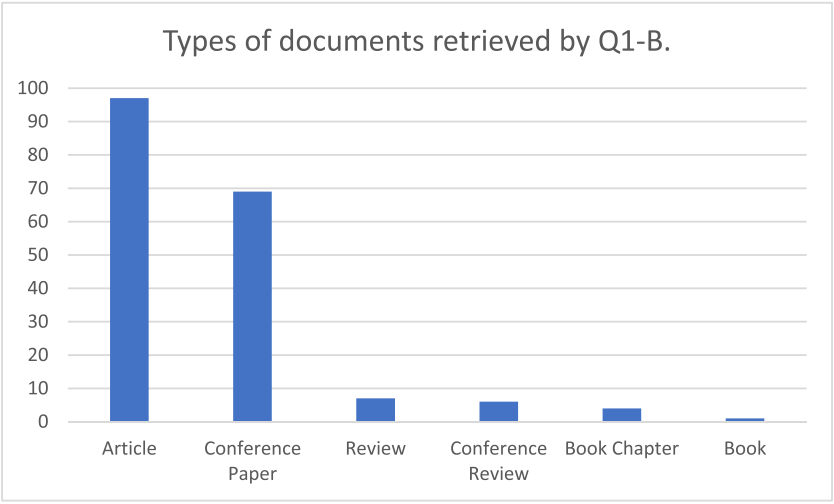

Fig. 3. Types of documents retrieved by Q1-B.

analyzed here (published between 1985 and 2022) have focused on the topics mentioned above.

It can also be seen that the publications about reinforced concrete (yellow circle) also refer to *corrosion*, *corrosion rate*, *chloride-induced corrosion*, and *failure analysis*. In turn, building materials and degradation (red circles) have been related to the preservation of cultural heritage and historic buildings, electrochemical corrosion tests, and atmospheric pollution (in green).

To provide a clearer view of the links between degradation and deterioration and other keywords found with Q1-B (as shown in Fig. 4), we zoomed in on them in Fig. 5. The analysis revealed that degradation is primarily associated with building materials and reinforced concrete, as well as atmospheric pollution, historic preservation, mortar, and cultural heritage, among others. On the other

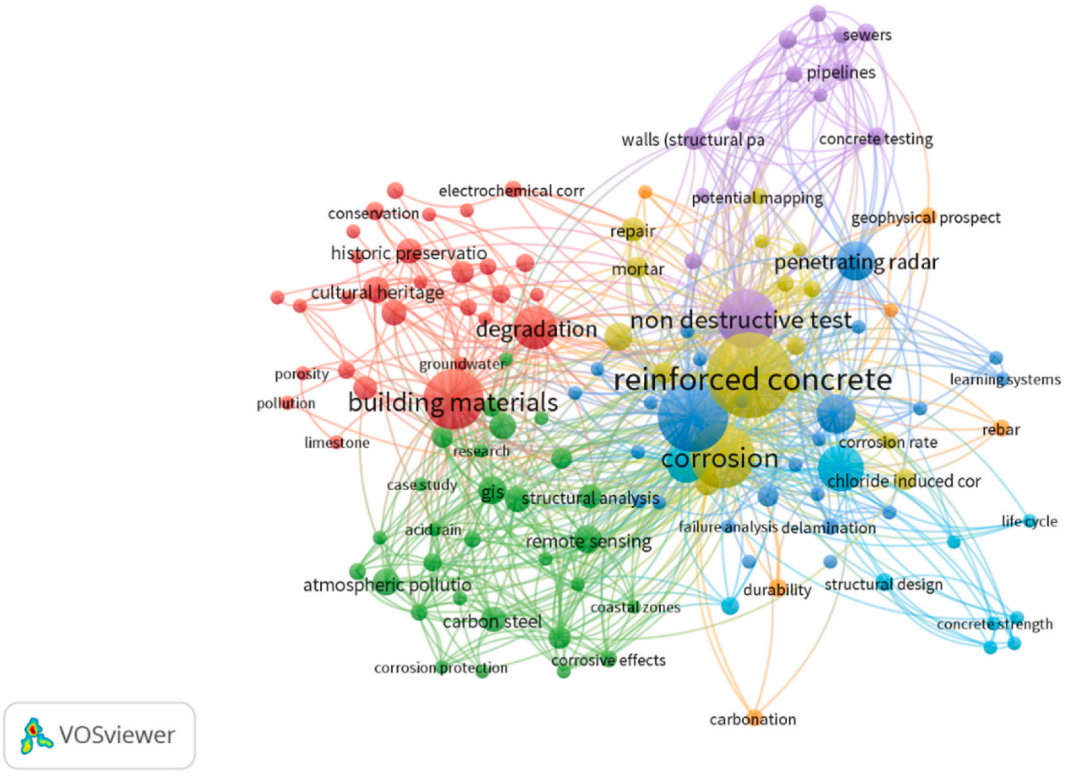

Fig. 4. Keyword network produced by Q1-B.

hand, deterioration is a more widely used term and is linked to degradation, pipelines, bridges, durability, carbonation, cracks, and repair.

4. Atmospheric degradation of ceramic building materials

Atmospheric pollution is an aggressive agent that can cause material deterioration, and despite being a current issue, it has existed since ancient times [7]. Nowadays, there are several aggressive agents that affect the durability of building materials, especially

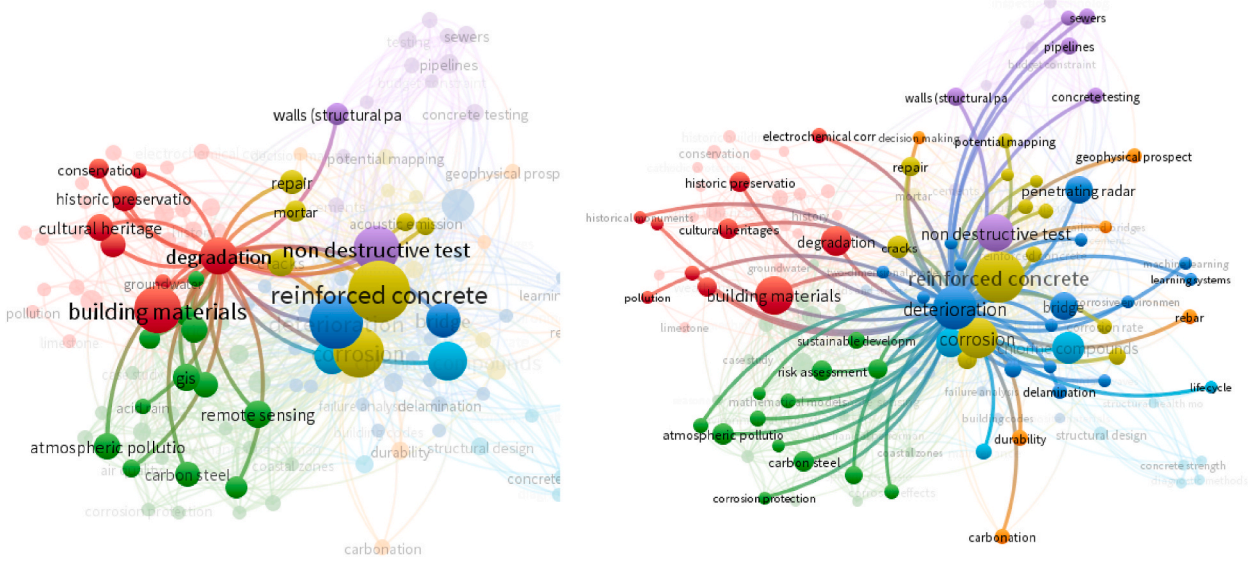

Fig. 5. Links of *degradation* and *deterioration* with other keywords.

structural concrete, such as carbon dioxide (CO_2), sulfate compounds, and chloride ions [8]. The degradation of ceramic materials in the atmosphere is characterized by the development of cracks, material undermining, hollowing, discoloration, and other effects caused by various climatic and environmental factors that affect their quality [9].

The deterioration process of ceramic building materials is a complex interaction with external environmental factors, including climatic conditions, local meteorological characteristics, biological processes, and challenging chemical processes resulting from pollutants and environmental elements. Moisture, temperature, solar radiation, airflow, pressure, precipitation, chemical and biological attacks, air movement, and pressure are key environmental elements that affect material deterioration [10].

Some authors provide examples of how landscapes around the world have deteriorated due to environmental factors. For instance, in Sao Paulo, Brazil, researchers discovered that pollutants and salts accumulate on walls, and gaps in a building's structure collect and retain moisture, leading to drainage displacement. Carbon nanotubes, fullerenes, and polycyclic aromatic hydrocarbons are particularly abundant in carbonaceous particles, which exacerbate the negative effects on human health and building materials. On average, 85% of particulate matter (PM) has the most negative impact on both human health and building materials, with Pb and Ti present in 56% of samples [11].

Gaowen et al. [12], To demonstrate the effect of sulfate-rich environments on concrete, studies have shown that sulfate attack causes significant weight loss and expansion in the later stages of corrosion, posing a serious threat to concrete structures. It has also been demonstrated that precast concrete exhibits greater resistance to sulfate attack than cast concrete, making it a preferable option for structures in service in sulfate-rich environments [12].

Researchers in Taiwan have discovered that fungi, plants, and microorganisms can cause deterioration in ceramic materials by invading their roots and hyphae, leading to serious harm to internal structures. Additionally, they found that ceramic materials are highly vulnerable to weathering in coastal areas [13].

4.1. Chloride-induced corrosion

According to numerous authors from around the world, chloride ions are the most prevalent and significant atmospheric corrosive agent. The rate of atmospheric corrosion is accelerated by atmospheric salinity [14]. Chloride ions directly participate in electrochemical corrosion reactions and also create electrolytes that are aided by hygroscopic salts like NaCl and $MgCl_2$ [15,16]. The deposition of these salts on the surface of materials increases rapidly for aerosols larger than 20 μm, and for 100-μm aerosols, it is approximately four times faster [17]. The size and shape of pieces or structures are also important. For example, in the case of complex shapes such as those of buildings, said deposition varies along the structure and is higher at the edges of the structure, where there is more turbulence [18].

The transportation of chloride in concrete exposed to a marine environment is influenced by the intrinsic behavior of concrete as well as the exposure conditions. Moreover, the design of the mixture and the curing conditions determine the performance of concrete. The microstructure can be densified, and the binding ability of concrete can be improved to reduce the penetration of chloride ions by decreasing the water-to-binders ratio, incorporating pozzolanic materials, and prolonging the curing time [19].

The researchers [20]; found that the effect of chlorine ions is more prevalent in maritime environments, and it can largely influence iron locally, especially in the presence of low water/cement ratios and little rainfall. This localized corrosion causes uneven damage to the section, which also increases the focus of triaxial efforts on the structure's durability [21,22].

E. Correa et al. [23] demonstrated in their study of the deterioration of concrete in various locations that the area with the highest corrosion rate had the greatest quantity of chloride ions, followed by the area with the highest concentration of CO_2.

4.2. Sulfate-induced corrosion

Hydrogen sulfide (H_2S), sulfuric acid (H_2SO_4), sulfur dioxide (SO_2), sulfur trioxide (SO_3), and salts of sulfuric acid are all sources of sulfates. Sulfur dioxide (SO_2), which is produced by burning sulfur-containing fossil fuels, is the primary cause of corrosion from these compounds. In urban and industrial atmospheres, the impact of sulfur dioxide is particularly significant for atmospheric corrosion [24,25]. The oxidation of sulfur dioxide produces sulfate ions in the surface moisture layer, according to Equation (1) [16]:

$$SO_2 + O_2 + 2e^{-} - > SO_4^{2-} \quad (1)$$

Sulfate attacks may lead to variations in the mechanical properties, interface binding, cracks, microstructure, and composition of concrete [26]. These attacks can generate expansive products and the decomposition of the products of cement hydration [27].

Researchers have found that when an SO_4^{2-} ion enters the concrete, it reacts with the calcium hydroxide, tricalcium aluminate, or the hydration products in the aluminum phase to produce expansion products such as ettringite, mirabilite, and gypsum. This reaction can lead to the destruction of the internal structure of the material [28–30].

An important deterioration process in these materials is "sulfation." It occurs when high concentrations of sulfates come into contact with the hydrated compounds of cement paste. This contact produces a chemical reaction that generates expansion in the paste and pressure that can break it, ultimately leading to the disintegration of the concrete [9]. This results in a volume increase in the solid, and, according to the reaction with the components of cement, can otherwise generate cracks and softening in the concrete.

When exposed to external sulfates, the structural elements of concrete deteriorate due to the formation of expansive phases such as ettringite and gypsum, leading to the dissolution of portlandite [31]. Wu et al. [32] have shown that as sulfate ions permeate the concrete matrix, the concrete undergoes significant deterioration, including cracking and spalling. This ultimately leads to a decrease

in the concrete's strength and an increase in its permeability [32,33].

4.3. Carbonation

CO_2 is a natural component of the atmosphere, but its content has significantly increased (more than 14%) since the start of this century, mainly by human activity (industrialization, road traffic, wildfires, etc.) [7].

Higher levels of CO_2 and temperature have been found to increase the likelihood of corrosion induced by concrete carbonation [6]. This carbonation process can also be caused by the oxidation of carbon monoxide, which is generated during incomplete combustion of carbon and hydrocarbons in heating systems or thermal power stations. Although carbon dioxide has limited solubility in water, the small portion that is dissolved can produce carbonic acid [7]. When CO_2 combines with raindrops, it forms carbonic acid, which is a constituent of acid rain. The pH of this type of rain is lower than 5.6, making it more aggressive towards ceramic materials and, more importantly, towards cultural heritage buildings [7].

In cement, the carbonation process has little consequence. However, in concrete, this chemical process advances slowly and progressively towards the inside of the exposed surface of the concrete and reaches the steel reinforcement, causing its corrosion [9], as shown in Fig. 6. During carbonation, the material's pH value, which was initially high during the pore solution phase, is lowered to a point where the passive layer can break, allowing the steel to corrode [23,34].

The degree of carbonation in concrete depends on several factors. According to Abd Elmoaty [21], the concrete compressive strength and porosity significantly affect the rate of carbonation. Additionally, the depth of carbonation is reduced when the cement concentration is increased, with an average reduction of 4 mm in carbonation depth when cement content is increased from 350 kg/m^3 to 450 kg/m^3. This indicates the influence of temperature and humidity on carbonation as well.

According to Guofang Chen et al. [6], climate change is expected to have a significant impact on carbonation rates, leading to higher ultimate carbonation depths in the long term. As a result, structures may require maintenance earlier than expected. The authors also found that in China's extreme cold, cold coastal, and temperate coastal temperature regions, climate change could result in an additional 20–160% of carbonation-induced damage to concrete structures by the end of this century.

4.4. Frost attack

Concrete is susceptible to frost attack damage due to its ability to absorb and maintain humidity, particularly in nations where the air temperature falls below 0 °C [35]. According to Joseph J. Assaad et al. [36], when water freezes, it expands by around 9% in volume. This expansion causes the formation of internal micro-cracks in the concrete due to the application of tensile stress on the area containing frozen water. These micro-cracks create a surface that can absorb water by capillarity, resulting in a progressive escalation of the cracks until the concrete is completely deteriorated [36].

Ceramic materials have a porous structure with pores that can vary in size by several orders of magnitude. The properties of the pore surfaces can affect the structure of water in the pores, which can exist in various forms, such as macroscopic ice, structured or pre-structured water [37]. Due to this complexity, a significant volume of mobile, non-frozen water can remain in the pore system of ceramic materials even when exposed to freezing temperatures. This can lead to transportation processes and contraction effects.

David Martín Freire Lista et al. [38] conducted research on granite used in the creation of Spanish heritage sites and found that when exposed to freeze-thaw cycles, it leads to differential microcracking, surface crystal loss, and ultimately decomposition. Unlike more ductile materials, quartz granites showed microcracks within the grain when exposed to ice-thaw cycles.

4.5. Acid attack

Ceramic materials that have acidic characteristics are prone to attack by basic mediums. For instance, ceramics made of SiO_2, which is acidic, can be attacked by NaOH solutions. Similarly, basic ceramic materials such as MgO can be attacked when they come into contact with acidic media [39].

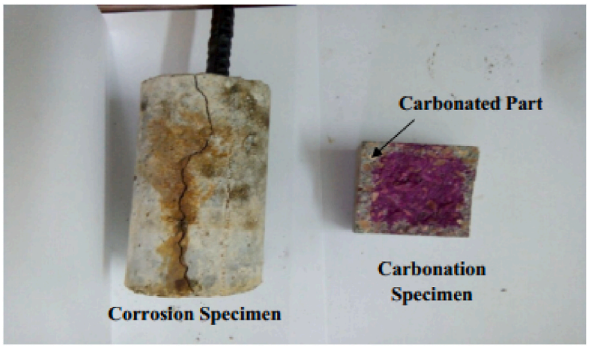

Fig. 6. Carbonation and corrosion specimens [21].

In general, concrete cannot withstand acid attacks, except for those caused by slightly acidic solutions. An acid attack results in the conversion of calcium compounds (such as calcium hydroxide, dihydrate calcium silicate, aluminum silicate, and hydrate calcium) into classic salts of the acid. When these salts are soluble, they can be displaced, which increases the porosity of the material and destroys its structure [9].

In their study, S. Gibeaux et al. [40], investigated the impact of acid attacks on natural and artificial stones used in architectural finishing. The dissolution of calcite and sulfates in all types of stones was found to be the main factor leading to material loss. The study also highlighted the importance of the pore size of the material. The authors used a synthetic acid solution that was more aggressive than actual rainwater, suggesting that the effect of acidity might be more significant than that of karstification.

4.6. Influence of water (acid rain, seawater)

Acid rain is a highly corrosive medium that contains additional species such as NH^{4+}, Mg^{2+}, and SO_4^{2-} in addition to H^+. As a result, the mechanisms of acid rain attack on cementitious materials are significantly different and more intricate than those of pure acid attack. Acid rain causes physical and chemical changes in concrete, which lower the pH value of the structure. The ongoing reaction gradually reduces the mechanical strength of the concrete structure, leading to cracking, mass loss, and ultimately, structural failure [41].

Zheng S et al. [42] investigated the effects of acid rain on the mechanical behavior of brick masonry. They observed that during the initial stages of acid rain disintegration, the surface of the mortar prism showed signs of sandblasting and white crystal spots. In the middle stage of acid rain corrosion, the color of the mortar prism's surface changed, and the "skinning" phenomenon became apparent. At the end of the corrosion process, the "skin" phenomenon on the mortar prism's surface worsened, and in some places, it started to peel off. The compressive strength of the brick decreased from 16.37 MPa to 13.06 MPa (20.22%) after 300 cycles of acid rain weathering.

The researches show the reactions define the corrosion process for a typical Portland cement paste specimens under acid rain attack [41]:

$$2H^+ + Ca\,(OH)_2 \rightarrow Ca^{2+} + 2H_2O \tag{2}$$

$$H^+ + C-S-H \rightarrow Ca^{2+} + SiO_2.nH_2O \tag{3}$$

$$H^+C-A-H \rightarrow Ca^{2+} + Al_2O_3.nH_2O \tag{4}$$

$$SO_4^{2-} + Ca^{2+} + H_2O \rightarrow CaSO_4.2H_2O \tag{5}$$

$$H^+ + 3CaO.Al_2O_3.CaSO_4.32H_2O \rightarrow Ca^+ + CaSO_4.\,2H_2O + Al_2O_3.nH_2O \tag{6}$$

Were.

$Ca(OH)_2$: Calcium hydroxide
(C–S–H): hydrated silicate calcium
(C-A-H): hydrated aluminate calcium
($CaCO_3$): calcium carbonate

The chemical reactions in Eqs. (2)–(6) implies that, during an acid rain attack, the hydrated products of regular cement, such as Ca $(OH)_2$, C–S–H, x$CaOAl_2O_3$-, and H_2O (abbreviated as CxAHy or C-A-H), gradually decompose into a mixture of carbonated, soft, and white corrosion products that are primarily composed of crystals of $CaSO_42H_2O$, SiO_2nH_2O gel, and Al_2O_3n [41].

4.7. Cracking

Temperature variations can create a thermal gradient between the outermost surface and the internal layer of a material, particularly in those with lower heat conductivity. This can result in the deterioration of the material's mechanical properties and the development of small cracks. The formation of fractures can cause a loss of material strength and an increase in porosity, which can further reduce the material's chemical resistance. Temperature fluctuations can also affect the bulk expansion of a material, including the expansion of stone grains, the dilation of different materials at joints, and the expansion of water in material capillaries. In tropical and subtropical regions, the rate of wet deposition is more significant for deterioration processes due to the higher ambient air temperature, while the impact of freeze-thaw cycles is less pronounced [10].

Particles have a higher chance of adhering to a damp surface, and water-soluble gases are more likely to be trapped. When condensation occurs on the surface of a material, both gas and particle fluxes increase, while they decrease during evaporation. Surface pollutants undergo chemical and photochemical reactions in a moisture layer, which also serves as a conductive channel for electrochemical reactions. Most materials deteriorate faster at higher relative humidity because it prolongs the wetness period, accelerates pollutant deposition, and creates favorable conditions for biodeterioration [10].

The wind's impact on ceramic aging is due to its ability to transport liquid and solid particles from the atmosphere to the material's surface, leading to erosion and accelerating weathering. The kinetic energy of the particles and wind speed can influence how droplets

impact the surface. Abrasion and diffusion are influenced by the high and low ends of the wind spectrum, respectively. Additionally, wind flows adjacent to a building can impact the rate of gaseous and particle pollution deposition and the force of driving rain in an area [10].

5. Monitoring and evaluation

5.1. Measures to monitor harmful substances in the aggregates

The expansive products of this reaction seek out spaces within the microstructure of concrete, the paste-aggregate interface, and the porosity of the aggregate, which generates internal tension. This tension leads to expansion and, consequently, the deterioration of the elements, as observed in Fig. 7 [43].

To determine the ASR potential of aggregates, the Colombian standard NTC 175 or its American equivalent (ASTM C289) can be used. These standards determine the reactivity of the aggregates by subjecting them to a solution of sodium hydroxide at 80 °C for 24 h and measuring the amount of alkalies that react with the solution. This test helps to identify the potential for ASR in concrete mixtures containing the tested aggregates [44]. To determine the potential reactivity of the cement-aggregate combination, either ASTM C227 or the Colombian standard NTC 3838 can be used. These standards help to determine the susceptibility of cement-aggregate mixtures to expansive reactions involving hydroxyl ions linked to alkalies by measuring the increase (or decrease) in the length of mortar bars containing the combination during storage under the specified test conditions of 38.2 °C and 50% humidity. The test evaluates the presence of sodium and potassium ions in the mixture, which can cause expansive reactions [45].

We can apply the procedure outlined in ASTM C586 (rock-cylinder method) to determine the possible alkali reactivity of specific carbonated rocks that can be used as concrete aggregates. In the latter, the change in the length of the cylinder is evaluated while stored in an alkaline solution. If the cylinder presents an expansion $\geq$0.1% after 84 days of testing, it is considered potentially reactive [46].

5.2. Electrochemical measures of corrosion

Electrochemical methods, such as electrochemical impedance spectroscopy (EIS) and linear polarization resistance, are commonly used to assess the condition of rebars. These methods can determine the polarization resistance (Rp) value of the system being studied. The corrosion current density (Icorr) is inversely proportional to the polarization resistance and directly proportional to the corrosion rate (Vcorr) [47,48].

The electrochemical behavior of steel can be assessed by routinely measuring the corrosion potential, polarization resistance (Rp), and corrosion current density (Icorr) using a potentiostat/galvanostat, a reference electrode, and a counter electrode on a weekly or monthly basis. These analyses should be conducted on both the exposed and non-exposed faces of the steel, and any differences between them should be evaluated [49].

In general, to determine electrochemical impedance, we use an electrolyte, which can be deionized water or a solution to be examined, along with a saturated calomel electrode (SCE) as a reference electrode and a platinum wire or plate as a counter electrode. The probes should be left inside the electrolyte for 30 min before each measurement to stabilize the potential, and measurements are then made within a predetermined scanning frequency range [23].

Electrochemical measurements can also be taken in situ. For that purpose, after curing the test samples, two different sensors are incorporated into each sample of concrete to assemble some electrochemical parameters, such as the corrosion potential of this material [5].

5.3. Analysis of structures using a carbonation test

The accelerated test is conducted in a carbonation incubator at a specific temperature and humidity, depending on the phenomenon being studied, and a given CO_2 concentration. After a certain time, a slice of the specimen, with a specified thickness, is extracted, and the depth of carbonation is measured using phenolphthalein as an indicator. Following the full exposure time, the permeability to liquid water, contact angle of water, and thickness of the equivalent air layer are evaluated in the concrete specimens [50].

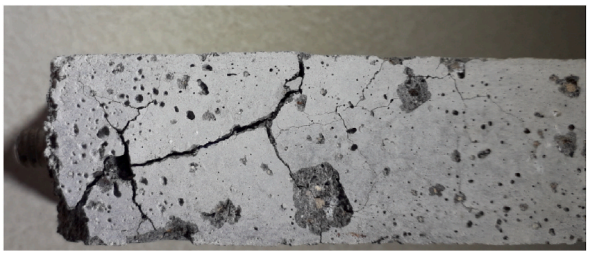

Fig. 7. Cracks produced by the reaction between cement and aggregates [43].

5.4. Chloride content

To determine the chloride content, we can use the capillary absorption method (the Fagerlund method) and the test method for measuring chloride ion penetration (ASTM C1202) [49]. However, there are other methods that can be used to determine the amount of free chloride, such as free chloride determination. To perform this method, 5 g of the material is mixed with 50 ml of distilled water and then subjected to lixiviation. The mixture is stirred vigorously, filtered, and the pH of the filtrate is measured with a pH meter. The filtrate is then dried in an oven for 24 h at 100 °C after being rinsed numerous times with distilled water. X-Ray fluorescence (XRF) spectroscopy is used to assess the chloride content of the filtrate, and the difference between this value and the total chloride content is used to determine the amount of free chloride in the original mass [5]. According to the UNI 9944 standard and Tittarelli et al. [51], the total chloride content is represented as a percentage of the total binder weight, and some examples are shown in Table 2.

5.5. Permeability and porosity tests

The deterioration process of Portland cement begins with the hydration products, mainly $Ca(OH)_2$ and the *C*–S–H gel. Once all the available $Ca(OH)_2$ has been consumed and the cement matrix has dried, the resulting calcium carbonate converts into soluble bicarbonate and gets leached out. Consequently, the set cement becomes more porous and permeable, leading to a decline in its compressive strength [53]. Table 3 presents some examples of porosity percentage.

An axial helium porosimeter and an axial air permeameter can be used to respectively measure the porosity and air permeability of concrete. These tests are conducted across the full surface area of concrete samples, including their entire base. The same analysis is performed on both treated and untreated specimens [53]. Concrete's oxygen permeability can be determined using the procedure outlined in the UNE 83981 (2008) standard for concrete durability test procedures. It is recommended to measure the concrete's hardened gas permeability [57,58].

Additionally, the EN 1062-3 standard can be used to quantify the liquid water permeability coefficient (also known as the capillary water absorption coefficient, C) [43]. The capillary water absorption phenomena are the main focus of this test. Cylindric specimens with varied heights and a diameter of 8 cm are made for the test. While the other's face is waterproofed with epoxy resin, just one of their faces has been treated with water repellent. The treated face is immersed in water that is 5 mm ± 1 mm, and the sample is weighed after 10, 30, 1, 2, 3, 6, and 24 h. Utilizing data collected after 24 h, the liquid water permeability coefficient is determined Eq. (7), where Δm24 it is the difference in specimen mass (kg) between zero and 24 h of immersion, and A is the specimen's contact area. (m^2) [50].

$$w = \frac{\Delta m_{24}}{\sqrt{24\ x\ A}} \left[\frac{kg}{m^2 h^{0.5}}\right] \tag{7}$$

5.6. Freeze-thawe–thaw test

Several researchers have conducted experiments on mortars to evaluate their performance under freeze-thaw conditions. The specimens were first removed from their molds and soaked in water at a specific temperature for a predetermined period. Subsequently, they were placed in a controlled climatic chamber under predetermined temperature, humidity, and time conditions. Reference specimens were also prepared and placed under the same conditions as the test specimens, but without exposure to freeze-thaw cycles. The testing specimens, on the other hand, were subjected to a total of 56 cycles of freeze-thaw.

Typically, a single freeze-thaw cycle lasts for a duration of 24 h. It is necessary for the internal temperature of the specimen to remain above 0 °C for a minimum of 7 h and not exceed 9 h during this period. The temperature range for the cycle should be within −20 ± 2 °C at its lowest and 20 ± 4 °C at its highest. The duration of the freezing period should be 16 h, while the thawing time should be 8 h [4].

5.7. Compressive tests

In this section, we will discuss the results obtained by the authors in their study on the degradation of ceramic construction materials with continuous performance, using mechanical tests. The compression test is the most commonly used method for evaluating deterioration and, therefore, receives additional attention in this study.

Table 2
Chloride ion content examples in ceramic construction materials.

Material	Chlorides content	Conditions	Reference
Ordinary Portland Cement (OPC)	3.1 (wt.% of binder)	Total chloride concentrations at 10–20 mm depth after 12 wet-dry cycles in 3.5% NaCl solution.	[51]
Reference concrete with aggregates based on silica	14.9 ± 1.8 (wt.%)	Evolution of the coefficient of migration of chlorine ions according in 180 days for concrete	[52]
Concrete	0.6 g of total chlorides per kilogram of concrete.	concrete prisms specimens with dimensions of 40 × 30 × 15cm^3, between 250 and 300 days	[5]
Coral coarse aggregates Coral	0.025	In concretes with OPC	[48]

Table 3
Porosity percentage examples in ceramic construction materials.

Material	Porosity (%)	Conditions	Reference
OPC	25	Total porosity (Vp) of OPC after 28 days of curing	[51]
Reference concrete with aggregates based on silica	11.2 ± 0.7 to 11.9 ± 0.3	Evolution of water porosity over 35 days–180 days for concrete	[52]
Concrete (name by authors as M1)	8.41	Effective porosity measured by computed tomography (CT)	[54]
Concrete (name by author as Paste RT OPC)	30	Porosities determined by the solvent exchange method using acetone.	[55]
Concrete with natural coarse aggregate	15.9	Porosity of concrete with chloride ion corrosion for 90 days	[56]
Concrete with recicled coarse aggregate	21.2	Porosity of concrete with chloride ion corrosion for 90 days	[56]

In a study by Zhao et al. [53], the resistance of concrete against sulfate attack was investigated, and it was observed that the concrete's performance was significantly influenced by the water/cement ratio, both in terms of compressive strength and resistance against sulfate attack. It is widely accepted that the density of concrete is substantially higher and its porosity is lower when the water/cement ratio is lower. Therefore, specimens with a lower water/cement ratio exhibited comparatively higher compressive strengths. Furthermore, the porosity of concrete plays a crucial role in determining the rate of sulfate ion diffusion, which ultimately affects the mechanical properties of the material [12].

Zu et al. [22], discovered that the ultimate strain of a steel reinforcement exponentially decreased as a result of corrosion until it stabilized, up to a certain threshold level (30% mass loss). The ductility of the corroded steel reinforcement was considerably impacted by the corrosion morphology. Additionally, the concrete's properties also played a significant role in determining the performance of the corroded steel reinforcement.

The mechanical behavior of concrete is commonly evaluated using several standard methods. The ASTM C39 standard is used to determine the compressive strength of concrete specimens at 28 and 90 days. The ASTM C496 standard is utilized to measure the splitting tensile strength of the concrete. Additionally, the modulus of elasticity of the concrete can be determined using the ASTM C469 standard [49].

Abd Elmoaty M [21] presented experimental results that confirm the detrimental impact of sulfate-contaminated aggregates on the four-year compressive strength of concrete. The study aimed to investigate the effect of different aggregate types used in concrete production and their response to deterioration. The results indicated that magnesium sulfate-contaminated aggregates had the most adverse effect compared to aggregates contaminated with sodium and calcium. However, by using a lower water-cement ratio, higher cement content, and Type V Portland cement, the four-year compressive strength of concrete can still be improved when using sulfate-contaminated aggregates.

In their study Gaowen Zhao et al. [12] observed that concrete strength started to decrease early when the water/cement ratio was higher, and the strength was relatively low towards the end of immersion. The researchers found that the concrete's strength decreased more rapidly and lost more strength when immersed in the solution with the highest sulfate concentration. The study illustrated how the water-cement ratio and sulfate-containing solutions influenced the compressive behavior of concrete mixes with different curing timeframes.

6. Degradation maps of ceramic building materials

One approach to reducing the expenses related to structural deterioration is to comprehend how the atmospheric environment influences materials that are exposed to it during their service [59]. Furthermore, generating maps of corrosion rates for building materials can help in identifying regional disparities in the intensity of corrosion processes in cities and countries.

Oliveira et al. [11], investigated the impact of pollutants on buildings and historical heritage and concluded that high concentrations of atmospheric pollutants, primarily generated by a significant number of motor vehicles, are a key contributor to the corrosion-induced deterioration of buildings and historical structures. They recommended strategies for preserving historical heritage, such as monitoring the pollution of structures and performing periodic restoration efforts [11].

The analysis of atmospheric deterioration of concrete can be carried out by exposing cylindrical [23] and prism [50] specimens to different atmospheric conditions of interest, and monitoring them over time. Carbonation, porosity, and compressive strength tests can be conducted to investigate the changes in the properties of the material due to deterioration [21]. In addition, many authors have investigated the effect of deterioration on reinforced concrete using electrochemical tests. The results of these tests can be compared with the levels of pollutants in the atmosphere to determine the aggressiveness of a specific atmosphere and develop deterioration maps for this material.

To minimize directional bias when testing limestone samples, it is recommended to place them on rotating supports. The recession rates of the samples can then be determined by measuring their mass loss over time [25].

6.1. Statistical processing of information

To express the relationship between the corrosion or deterioration rate and the combined level or loads of pollutants and meteorological conditions, the dose-response function is a common approach [59]. Measurements of environmental factors such as temperature, relative humidity, gaseous pollutants (SO_2, NO_2, and O_3), or precipitation are typically collected from local environmental

stations or with the use of specialized measuring devices [59].

Some authors have utilized data modeling and tools, such as MULTI-ASSESS, to establish a dose-response relationship based on the results of the 8-year ICP-Materials field exposure program, which is an international program aimed at studying the deterioration of various materials in Europe. Their studies have investigated the link between air pollution, climate, and the deterioration of structural materials.

Some researchers have utilized multivariate predictive modeling techniques to study the relationship between air pollution and structural deterioration. For instance, a study was conducted to investigate pollution in the city of Rome by adopting a strategic focus on Partial Least Squares-Discriminant Analysis (PLS-DA). This method was able to identify the most relevant pollutants and their sources, as well as their impact on building materials. The results of this study could help in developing effective strategies for preserving the city's historical heritage [60].

Kriging interpolation is a method that can be used to estimate the aggressiveness of a site based on its proximity to other monitored locations. This technique takes into account both the distance and variability between known data points, allowing for accurate estimation of values in regions without monitoring stations. By deriving weights through kriging, highly precise and reliable estimates can be obtained [61].

Various authors have employed the Shapiro-Wilk test to evaluate the statistical distribution of data. Additionally, they utilized t-tests, Mann-Whitney tests ($M-$ W tests) for two samples, or Kruskal-Wallis tests (K–W tests) with Dunn's post-hoc analysis for more than two samples to compare the datasets. By calculating Pearson or Spearman correlation coefficients, the authors were able to assess the strength of the relationship between the variables being studied [62].

6.2. *Types of maps and software used to build them*

ArcGIS software is utilized to create four different types of maps that classify and categorize areas based on their climatic characteristics and the risk posed to cultural assets. These maps include climate maps, heritage risk maps, heritage maps, and patrimonial materials maps [13]. An example of a heritage climate risk map is presented in Fig. 8. The patrimonial materials map combines accumulated calculations with the climatological map to classify the various levels of failure risk for the materials under investigation and to evaluate the risks to historic sites in specific locations.

Maps of contaminants are commonly used to assess the concentration of pollutants in different locations. After gathering all necessary information from independent experiments or extrapolating from other studies that utilize dose-response functions, maps can be developed in GIS for various scenarios, including pollutants such as SO_2, O_3, NO_2, NOx, PM10, etc., as well as maps that

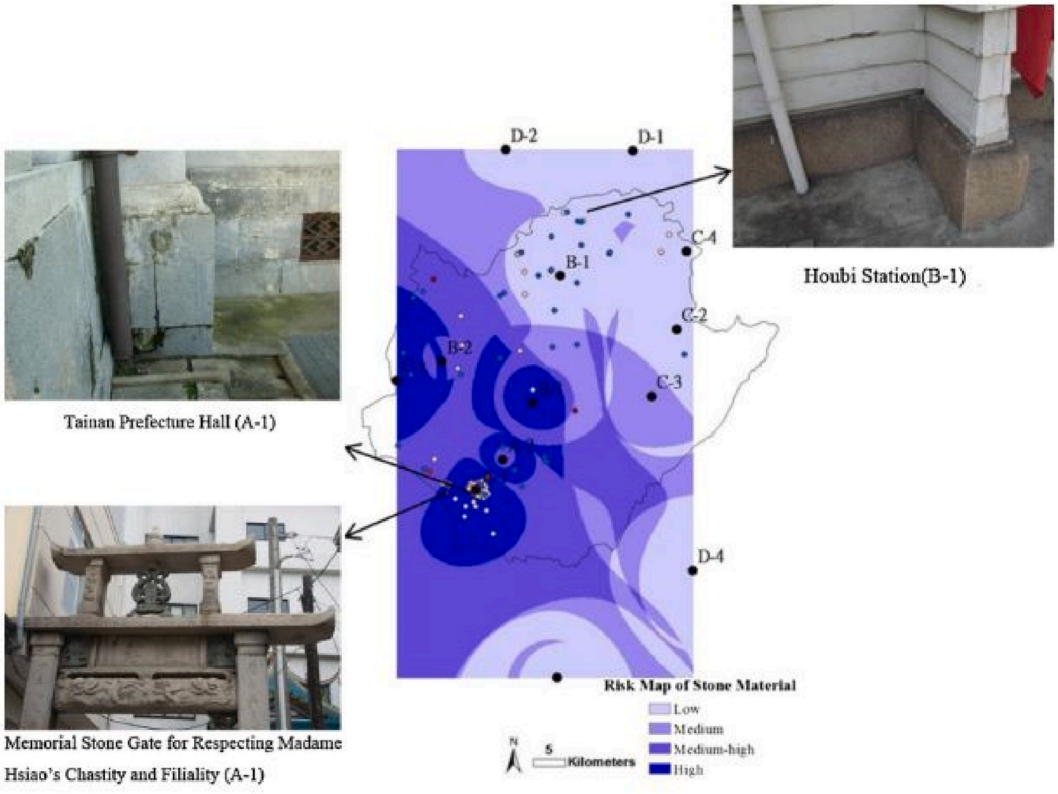

Fig. 8. Heritage climate risk maps for stone materials [13].

illustrate the overlap between corrosion and cultural heritage, the distribution of cultural heritage by material, the extent of corrosion by material, and the exceedance of tolerable deterioration criteria for each material [63].

Fig. 9 depicts a map of recession obtained using dose-response equations for Portland sandstone covering the period from 1995 to 2008. The map indicates a higher degree of recession in 1995. The generation of this map was achieved by implementing the MULTI-ASSESS framework that utilizes dose-response functions, in conjunction with the Kriging interpolation technique.

Various types of maps can be developed to analyze and visualize different aspects related to the study site. For example, atmospheric corrosivity maps can be created to determine the aggressiveness of each location within the study area, based on a classification system specified in the ISO 9223 standard [64]. Additionally, maps of corrosion, pollutant dispersion, temperature, critical relative humidity, historical climate, and cultural heritage can also be generated [13]. Corrosion maps can be produced for a specific material and time period or for the entire study duration, depicting the values derived from dose-response functions across the entire region. The process of creating these maps typically involves using tools such as MULTI-ASSESS and Kriging interpolation method [65].

Short-to medium-term climate maps illustrate the overall climate conditions in urban areas. Historical climate maps provide data on index elements that influence materials. Cultural heritage sites are typically identified on administrative maps using heritage maps that categorize them based on their historical significance. Additionally, atmospheric corrosivity maps can be created to evaluate the corrosive impact of a study site, based on classification criteria specified in ISO 9223. Corrosion maps for specific materials and time periods can also be generated using dose-response functions, to provide an assessment of corrosion levels across an entire region [13].

Regarding ceramic building materials, this review found climate, heritage risk, and stone recession maps. For example, Fig. 10 is a map of the recession of limestone in Slovakia [59]; Fig. 11, a map of the recession of limestone in Istanbul presented as a corrosion attack distribution map [66]; and Fig. 12, a map of the recession of limestone in Italy, which presents more moderate values than those in Slovakia [61].

6.3. Tolerable corrosion rates

According to a study [61], limestone surfaces in Milan, Italy corroded at a rate of 7–9.25 mm per year, which is higher than the acceptable corrosion rates for limestone in the region (4.8 mm per year for surface recession). Results from the ICP-Materials campaign between 1997 and 2001 showed a clear surface recession in unsheltered conditions, with an estimated loss of 20 mm over four years. In sheltered conditions, nearly 70% of tested locations showed surface gain, with a maximum increase of 6.6 mm, taking into account the effect of rain-wash-off [25].

For materials of a ceramic nature, it is common to generate resection maps that indicate their distribution in a specific region. The corrosion rate is defined as the amount of material loss that occurs within a set time period, typically measured in years. The degree of

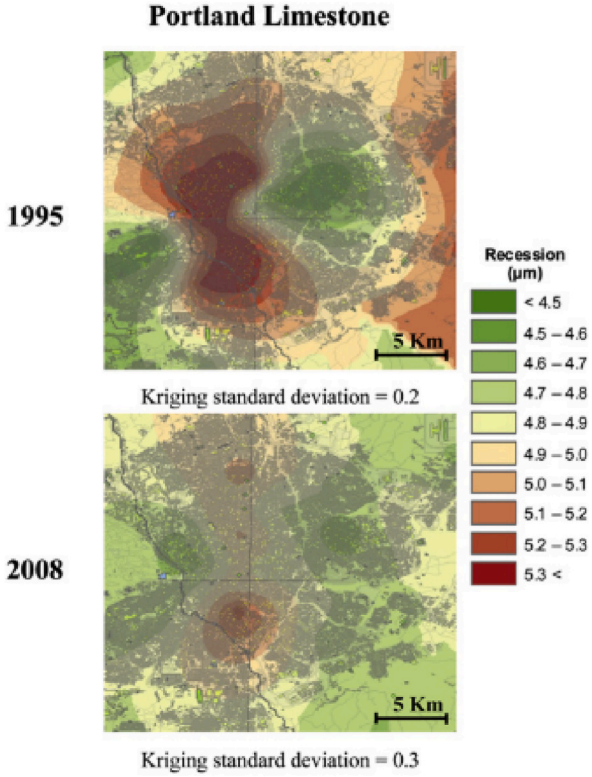

Fig. 9. Madrid, Spain's Portland limestone dose-response functions used to generate recession maps in 1995 and 2008 [63].

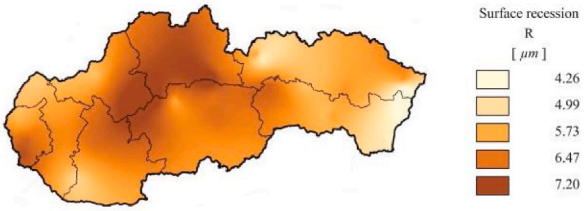

Fig. 10. Annual average surface recession of limestone for the first year of exposure in Slovakia [59].

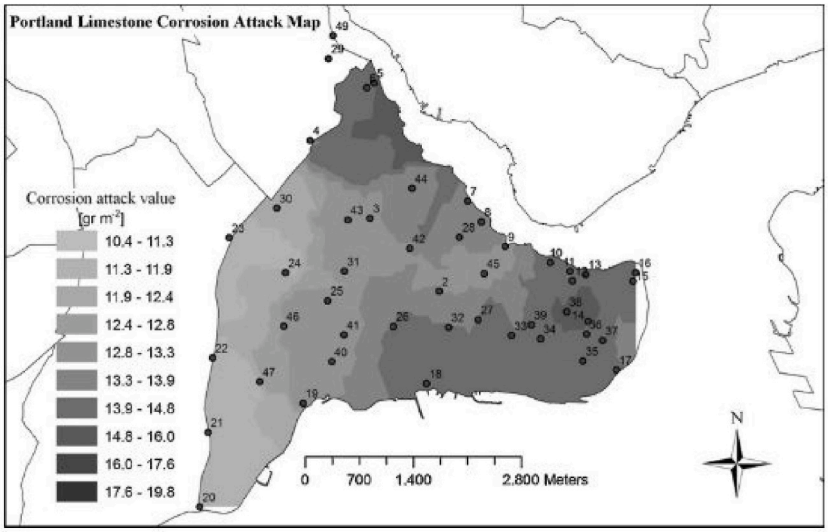

Fig. 11. Map of the distribution of corrosion effects on Portland limestone in Istanbul [66].

material loss is determined by the aggressiveness of the surrounding environment, which has been studied previously. Fig. 13 shows an Italian limestone resection map that is color-coded, with yellow indicating areas of lower material resection and red to brown indicating areas of greater material loss. This visual representation suggests that the environment is more hostile in the regions of the map that are colored in red to brown [67].

7. Discussion and future trends in the field of deterioration of ceramic building materials

Based on the bibliometric analysis conducted, it was found that current studies are related to the preservation of historical heritage, as well as the use of non-destructive and electrochemical testing methods. According to the review of forms of degradation of ceramic materials and the different tests that can be performed, it is important to explore the various forms of deterioration that occur in these materials. Furthermore, it is essential to conduct analyses beyond the materials used in historical heritage and to perform other available tests that aid in preventing and studying the degradation processes.

After conducting this review, it was found that trends in the study of ceramic material degradation are emerging, and some authors have already presented their opinions on future trends, which are outlined below.

Despite the significant role of climate change in the deterioration of monuments, there is a paucity of scientific research on this subject [67]. Climate change can accelerate or intensify some building deterioration processes while delaying others. Thermal stress caused by temperature fluctuations (daily, seasonal, or exceptional occurrences) can lead to façade deterioration, whereas wind can cause structural damage, surface erosion, and collapse [67].

Di Turo et al. [68] have developed models to predict future scenarios for the urban atmosphere in Europe in the year 2030, using data collected by international programs. Based on the chemical properties and reactions to pollution and environmental variables, they have found that metals are expected to be easier to conserve than limestones. Reductions in pollutant concentrations are crucial for material conservation, as improved air quality will mitigate metal corrosion and surface erosion."

According to some authors [66], a 50% reduction in pollution can lead to an average overall increase in short-term maintenance intervals due to atmospheric weathering of approximately 25%, resulting in maintenance cost savings of about 10%. However, the significance of atmospheric chemical weathering in comparison to other factors must be taken into consideration when refurbishment, rehabilitation, and maintenance interventions are carried out on exterior material surfaces and façades.

Karaca [66] employed MULTI-ASSESS dose-response functions to investigate the impact of air pollution-induced corrosion in

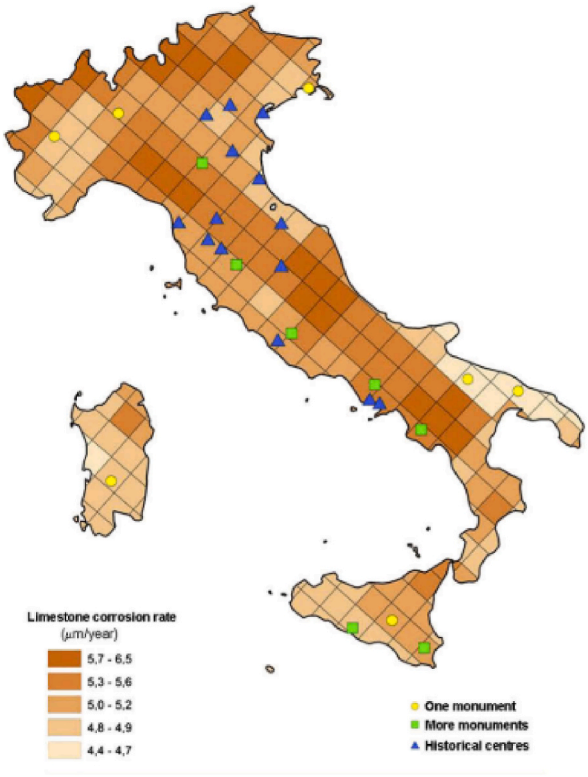

Fig. 12. Location of Italian UNESCO sites and multi-assess methodology for limestone corrosion rate presented as the surface recession in 2000 (EMEP data) [61].

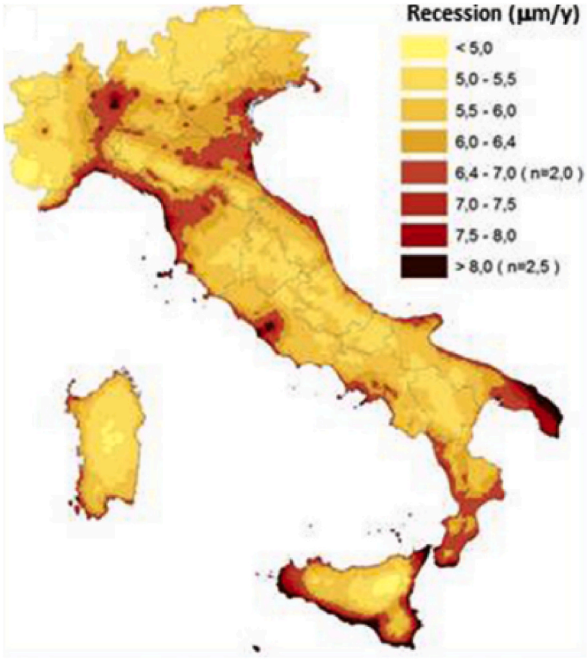

Fig. 13. Corrosion map for limestone in 2010 in Italian territory [67].

Istanbul and subsequently evaluated the data utilizing tolerated corrosion levels. The author found that the corrosion levels in carbon steel, copper, cast bronze, and limestone are higher than the 2020 targets, implying that the pollution levels must be reduced.

The primary focus of current research in the field is the development of nanomaterials to improve the mechanical properties of ceramic construction materials and protect them from deterioration and degradation. Various nanomaterials, including graphene oxide/platelets, carbon nanotubes, silver, copper, nano clay, titanium dioxide, nano iron oxide, nanosilica, and nanoclay, have been extensively discussed for this purpose [69].

The production of concrete requires strong and durable nanoparticles. Silica (SiO2) is a typical component of traditional concrete. However, the addition of nano-silica has been found to decrease concrete porosity, thereby reducing concrete deterioration. Two primary physical stressors, namely shrinkage and abrasion, can impair cementitious materials, leading to crack initiation and expansion throughout the cementitious material [70]. The performance of cement can be enhanced by incorporating nanoscale components into concrete. Addition of nano-SiO2 to concrete containing high volumes of fly ash can significantly improve the compressive strength by filling the nanoscale gaps between large fly ash and cement particles, especially when the concrete is still fresh [70].

Biodeterioration is one of the most critical characteristics of ceramic construction materials. Nano silica oxide-based antimicrobial coatings are commonly used to prevent the biodeterioration of stone surfaces and buildings [71]. In recent times, there has been an increased emphasis on using nanomaterials in cultural heritage preservation. Several recent examples include the application of nanomaterials to protect paper, glass, textiles, and stone monuments. Although nano-silver and nano-titanium-based products are commonly explored, several other readily available multifunctional nanomaterials have been demonstrated to function as alternatives to traditional remedies for legacy biodeterioration problems [72].

8. Conclusions

The bibliometric analysis conducted in this study revealed a very low number of scientific publications on the atmospheric deterioration of ceramic building materials, with only 184 documents published on this subject between 1985 and 2022. Most of the literature in this field has been authored by researchers in the United States and Canada, and the majority of publications are research and review articles, with only 5% being of a different kind.

The maps of keywords presented in this study reveal that the publications primarily investigated specific materials (e.g., reinforced concrete, mortars, building materials, and historical heritage) and topics (e.g., corrosion, atmospheric pollution, and heritage preservation). The deterioration tests in these studies mainly focused on studying mechanical properties, carbonation, and chemical properties using non-destructive testing.

This study provided a comprehensive review of the different atmospheric degradation mechanisms that affect ceramic building materials, including rebar corrosion, chloride-induced corrosion, sulfate-induced corrosion, carbonation, frost attack, acid attack, sulfation, the influence of water, cracking, and erosion. It also describes the general aspects of each mechanism and reviews recent studies that have investigated how different environmental factors affect this type of material.

Furthermore, this study defined basic concepts of monitoring and evaluation measures in the field of degradation of ceramic building materials, such as measures of harmful substances in concrete aggregates, electrochemical measures of corrosion, carbonation test, chloride content, permeability and porosity tests, freeze-thaw test, and mechanical tests. This can provide future researchers in this field with a general idea of how to define a measure of deterioration and thus provide tools to mitigate atmospheric damage to buildings and heritage.

Finally, it is important for materials researchers to design the structures of building materials in a way that their performance is not limited by changes in atmospheric and meteorological pollution parameters.

Author contribution statement

All authors listed have significantly contributed to the development and the writing of this article.

Data availability statement

The authors are unable or have chosen not to specify which data has been used.

Declaration of interest's statement

The authors declare no competing interests.

References

[1] R. Hamilton, H. Crabbe, Environment, pollution and effects, in: The Effects of Air Pollution on Cultural Heritage, Springer US, 2009, pp. 1–27, https://doi.org/10.1007/978-0-387-84893-8_1.

[2] C.P.J. Barrelas, Q. Ren, Implications of climate change in the implementation of maintenance planning and use of building inspection systems, J. Build. Eng. 40 (2021), https://doi.org/10.1016/j.jobe.2021.102777.

[3] International Concrete Repair Institute, A Vision for the Concrete Repair Protection and Strengthening Industry, 2004, pp. 1–29. Vision 2020.

[4] E. Menéndez, J. de Frutos, C. Andrade, Análisis no destructivo del estado de degradación en morteros bajo la acción de ciclos hielo-deshielo, Bol. la Soc. Esp. Ceram. y Vidr. 48 (5) (2009) 223–230.
[5] P. Romano, P.S.D. Brito, L. Rodrigues, Monitoring of the degradation of concrete structures in environments containing chloride ions, Construct. Build. Mater. 47 (2013) 827–832, https://doi.org/10.1016/j.conbuildmat.2013.05.042.
[6] G. Chen, Y. Lv, Y. Zhang, M. Yang, Carbonation depth predictions in concrete structures under changing climate condition in China, Eng. Fail. Anal. 119 (Jan. 2021), 104990, https://doi.org/10.1016/j.engfailanal.2020.104990.
[7] R. Fort, La contaminación atmosférica en el deterioro del patrimonio monumental: medidas de prevención, Cienc. Tecnol. Soc. para Una conservación Sosten. Patrim. pétreo (2007) 57–70.
[8] H. Torres, E. Correa, J.G. Castaño, F. Echeverría, Simplified mathematical model for concrete carbonation, J. Mater. Civ. Eng. 29 (10) (2017), 04017150, https://doi.org/10.1061/(asce)mt.1943-5533.0002001.
[9] F.J. Pancorbo, Corrosión, degradación y envejecimiento de los materiales empleados en la edificación, Marcombo, 2010.
[10] A. Moncmanová, Environmental factors that influence the deterioration of materials, in: Enviromental Deterioration of Materials, 2007, https://doi.org/10.2495/978-1-84564-032-3/01.
[11] M.L.S. Oliveira, et al., Air Pollutants and Their Degradation of a Historic Building in the Largest Metropolitan Area in Latin America, 2021, https://doi.org/10.1016/j.chemosphere.2021.130286.
[12] G. Zhao, M. Shi, M. Guo, H. Fan, Degradation mechanism of concrete subjected to external sulfate attack: comparison of different curing conditions, Materials 13 (14) (2020), https://doi.org/10.3390/ma13143179.
[13] P.S. Wu, C.M. Hsieh, M.F. Hsu, Using heritage risk maps as an approach to estimating the threat to materials of traditional buildings in Tainan (Taiwan), J. Cult. Herit. 15 (4) (Jul. 2014) 441–447, https://doi.org/10.1016/j.culher.2013.10.005.
[14] C.C. Lin, C.X. Wang, Correlation between accelerated corrosion tests and atmospheric corrosion tests on steel, J. Appl. Electrochem. 35 (9) (Sep. 2005) 837–843, https://doi.org/10.1007/s10800-005-1322-7.
[15] C. Vargel, The parameters of atmospheric corrosion, in: Corrosion of Aluminium, Elsevier, Paris, 2004, pp. 241–257, https://doi.org/10.1016/B978-0-08-099925-8.00040-5.
[16] S. Syed, Atmospheric corrosion of materials, Emirates J. Eng. Res. 11 (1) (2006) 1–24.
[17] I.S. Cole, D. Lau, D.A. Paterson, Holistic model for atmospheric corrosion Part 6 - from wet aerosol to salt deposit, Corrosion Eng. Sci. Technol. 39 (3) (Sep. 2004) 209–218, https://doi.org/10.1179/147842204X2880.
[18] I.S. Cole, T.H. Muster, N.S. Azmat, M.S. Venkatraman, A. Cook, Multiscale modelling of the corrosion of metals under atmospheric corrosion, Electrochim. Acta 56 (4) (Jan. 2011) 1856–1865, https://doi.org/10.1016/j.electacta.2010.10.025.
[19] Y. Yi, D. Zhu, S. Guo, Z. Zhang, C. Shi, A review on the deterioration and approaches to enhance the durability of concrete in the marine environment, Cem. Concr. Compos. 113 (Oct. 2020), 103695, https://doi.org/10.1016/j.cemconcomp.2020.103695.
[20] E.S. Josué Paredes, Juan Prieto, Corrosión del acero en elementos de hormigón armado: vigas y columnas, 2013.
[21] A.E.M.A. Elmoaty, Four-years carbonation and chloride induced steel corrosion of sulfate-contaminated aggregates concrete, Construct. Build. Mater. 163 (Feb. 2018) 539–556, https://doi.org/10.1016/j.conbuildmat.2017.12.128.
[22] W. Zhu, R. François, C.S. Poon, J.G. Dai, Influences of corrosion degree and corrosion morphology on the ductility of steel reinforcement, Construct. Build. Mater. 148 (Sep. 2017) 297–306, https://doi.org/10.1016/j.conbuildmat.2017.05.079.
[23] E. Correa, S. Peñaranda, J. Castaño, F. Echeverría, Concrete deterioration in Colombian urban atmospheres, Rev. Fac. Ing. Univ. Antioq. 52 (Mar. 2010) 41–46 [Online]. Available: https://revistas.udea.edu.co/index.php/ingenieria/article/view/14801/12954.
[24] J. Huang, X. Meng, Z. Zheng, Y. Gao, Effect of multi-pollutant state of ozone and sulfur dioxide on atmospheric corrosivity map of Guangdong Province, Environ. Pollut. 251 (Aug. 2019) 885–891, https://doi.org/10.1016/j.envpol.2019.05.073.
[25] F. Vidal, R. Vicente, J. Mendes Silva, Review of environmental and air pollution impacts on built heritage: 10 questions on corrosion and soiling effects for urban intervention, J. Cult. Herit. 37 (2019) 273–295, https://doi.org/10.1016/j.culher.2018.11.006.
[26] Y. Chen, P. Liu, Z. Yu, Study on degradation of macro performances and micro structure of concrete attacked by sulfate under artificial simulated environment, Construct. Build. Mater. 260 (Nov. 2020), 119951, https://doi.org/10.1016/j.conbuildmat.2020.119951.
[27] P. Liu, Y. Chen, Z. Yu, Z. Lu, Effect of sulfate solution concentration on the deterioration mechanism and physical properties of concrete, Construct. Build. Mater. 227 (Dec. 2019), 116641, https://doi.org/10.1016/j.conbuildmat.2019.08.022.
[28] K. Wang, J. Guo, H. Wu, L. Yang, Influence of dry-wet ratio on properties and microstructure of concrete under sulfate attack, Construct. Build. Mater. 263 (Dec. 2020), 120635, https://doi.org/10.1016/j.conbuildmat.2020.120635.
[29] J. Li, M. Shi, G. Zhao, Degradation and life prediction model for piles due to crystallisation attack in sulfate saline area, Adv. Cement Res. 32 (4) (2020) 181–195, https://doi.org/10.1680/jadcr.18.00147.
[30] A. Neville, The confused world of sulfate attack on concrete, Cement Concr. Res. 34 (8) (2004) 1275–1296, https://doi.org/10.1016/j.cemconres.2004.04.004.
[31] W. Müllauer, R.E. Beddoe, D. Heinz, Effect of carbonation, chloride and external sulphates on the leaching behaviour of major and trace elements from concrete, Cem. Concr. Compos. 34 (5) (2012) 618–626, https://doi.org/10.1016/j.cemconcomp.2012.02.002.
[32] J. Wu, J. Wei, H. Huang, J. Hu, Q. Yu, Effect of multiple ions on the degradation in concrete subjected to sulfate attack, Construct. Build. Mater. 259 (Oct. 2020), 119846, https://doi.org/10.1016/j.conbuildmat.2020.119846.
[33] William Garzón, Estudio de durabilidad al ataque de sulfatos del concreto con agregado reciclado, in: Trabajo de grado, Magister en Construcción Universidad Nacional de Colombia, 2013.
[34] P. Liu, Z. Yu, Y. Chen, Carbonation depth model and carbonated acceleration rate of concrete under different environment, Cem. Concr. Compos. 114 (Nov. 2020), 103736, https://doi.org/10.1016/j.cemconcomp.2020.103736.
[35] Y. Wei, W. Kong, Y. Wang, Strengthening mechanism of fracture properties by nano materials for cementitious materials subject to early-age frost attack, Cem. Concr. Compos. 119 (May 2021), 104025, https://doi.org/10.1016/j.cemconcomp.2021.104025.
[36] J.J. Assaad, F. Hamzeh, B. Hamad, Qualitative assessment of interfacial bonding in 3D printing concrete exposed to frost attack, Case Stud. Constr. Mater. 13 (Dec. 2020), https://doi.org/10.1016/j.cscm.2020.e00357.
[37] S. Palecki, S. Gorelkov, J. Wartmann, A. Heinzel, Frost induced damages within porous materials - from concrete technology to fuel cells technique, J. Power Sources 372 (Dec. 2017) 204–211, https://doi.org/10.1016/j.jpowsour.2017.10.065.
[38] D. Freire Lista, M. Varas Muriel, R. Fort González, Deterioro en el granito de Cadalso de los Vidrios bajo condiciones de Hielo/Deshielo, 2010, pp. 2008–2011.
[39] D.S. BF, Dr Ricardo Mario Carranza, Dr Gustavo Sergio Duffó, NADA ES PARA SIEMPRE. Química de la degradación de los materiales, Instituto Nacional de Educación Tecnológica, República Argentina, 2010. ISBN 978-950-00-0749-8.
[40] S. Gibeaux, C. Thomachot-Schneider, S. Eyssautier-Chuine, B. Marin, P. Vazquez, Simulation of acid weathering on natural and artificial building stones according to the current atmospheric SO2/NOxrate, Environ. Earth Sci. 77 (9) (May 2018), https://doi.org/10.1007/s12665-018-7467-6.
[41] M.C. Chen, K. Wang, L. Xie, Deterioration mechanism of cementitious materials under acid rain attack, Eng. Fail. Anal. 27 (Jan. 2013) 272–285, https://doi.org/10.1016/j.engfailanal.2012.08.007.
[42] S. Zheng, L. Niu, P. Pei, J. Dong, Mechanical behavior of brick masonry in an acidic atmospheric environment, Materials 12 (7) (2019), https://doi.org/10.3390/ma12172694.
[43] Asocreto, Como evitar la reacción alcalí del agregado, in: 360 en Concreto, 2020.
[44] N. Técnica, NTC 175 MÉTODO QUÍMICO PARA DETERMINAR LA REACTIVIDAD POTENTIAL ALCALI-SÍLICE DE LOS AGREGADOS, 1996.
[45] N. Técnica, MÉTODO DE ENSAYO PARA LA DETERMINACIÓN DE LA REACTIVIDAD POTENTIAL A LOS ÁLCALIS DE MEZCLAS DE CEMENTO-AGREGADO (MÉTODO DE LA BARRA DE MORTERO), 1996.
[46] E. 360, ASTM International - ASTM C586-11(2019) Standard Test Method for Potential Alkali Reactivity of Carbonate Rocks as Concrete Aggregates, Rock-Cylinder Method, 2019.

[47] E. Correa, S. Peñaranda, J. Castaño, F. Echeverría, Deterioro del concreto en ambientes urbanos de Colombia, Rev. Fac. Ing. 52 (2010) 41–46.
[48] D. Niu, L. Zhang, Q. Fu, B. Wen, D. Luo, Critical conditions and life prediction of reinforcement corrosion in coral aggregate concrete, Construct. Build. Mater. 238 (2020), 117685, https://doi.org/10.1016/j.conbuildmat.2019.117685.
[49] R. Verar, M. Villarroel, D. Delgado, A. Carvajal, F. De Barbieri, O. Troconis, Duracon: influencia de la acción del medio ambiente en la durabilidad del concreto, Rev. la Constr. 8 (1) (2009) 13–23 [Online]. Available: https://dialnet.unirioja.es/servlet/articulo?codigo=4282979.
[50] L. Courard, Z. Zhao, F. Michel, Influence of hydrophobic product nature and concentration on carbonation resistance of cultural heritage concrete buildings, Cem. Concr. Compos. 115 (Jan. 2021), 103860, https://doi.org/10.1016/j.cemconcomp.2020.103860.
[51] F. Tittarelli, A. Mobili, C. Giosuè, A. Belli, T. Bellezze, Corrosion behaviour of bare and galvanized steel in geopolymer and Ordinary Portland Cement based mortars with the same strength class exposed to chlorides, Corrosion Sci. 134 (Apr. 2018) 64–77, https://doi.org/10.1016/j.corsci.2018.02.014.
[52] A. Pichelin, M. Carcassès, F. Cassagnabère, S. Multon, G. Nahas, Sustainability, transfer and containment properties of concrete subject to delayed ettringite formation (DEF), Cem. Concr. Compos. 113 (Oct. 2020), 103738, https://doi.org/10.1016/j.cemconcomp.2020.103738.
[53] K. Sedić, N. Ukrainczyk, V. Mandić, N. Gaurina-Međimurec, J. Šipušić, Carbonation of Portland-Zeolite and geopolymer well-cement composites under geologic CO2 sequestration conditions, Cem. Concr. Compos. 111 (Aug. 2020), 103615, https://doi.org/10.1016/j.cemconcomp.2020.103615.
[54] G.L. Balázs, É. Lublóy, T. Földes, Evaluation of concrete elements with X-ray computed tomography, J. Mater. Civ. Eng. 30 (9) (Sep. 2018), https://doi.org/10.1061/(asce)mt.1943-5533.0002389.
[55] A. Mendes, J.G. Sanjayan, W.P. Gates, F. Collins, The influence of water absorption and porosity on the deterioration of cement paste and concrete exposed to elevated temperatures, as in a fire event, Cem. Concr. Compos. 34 (9) (Oct. 2012) 1067–1074, https://doi.org/10.1016/j.cemconcomp.2012.06.007.
[56] C. Chen, R. Liu, P. Zhu, H. Liu, X. Wang, Carbonization durability of two generations of recycled coarse aggregate concrete with effect of chloride ion corrosion, Sustain. Times 12 (24) (Dec. 2020) 1–19, https://doi.org/10.3390/su122410544.
[57] Susana Fernández García, Corrosión de armadura en el hormigón armado en un ambiente marino aéreo, Universidad politécnica de Madrid, Madrid, 2016. Accessed: April. 24, 2021. [Online]. Available: https://core.ac.uk/download/pdf/148679174.pdf.
[58] E. Del, D. Une, UNE 83981 (2008): Durabilidad del hormigón. Métodos de ensayo, Determinación de la permeabilidad al oxígeno del hormigón endurecido, 2008.
[59] M. Ivaskova, P. Kotes, M. Brodnan, Air pollution as an important factor in construction materials deterioration in Slovak Republic, Procedia Eng. 108 (Jan. 2015) 131–138, https://doi.org/10.1016/j.proeng.2015.06.128.
[60] A. Di Menno di Bucchianico, et al., Combined Effects of Air Pollution and Allergens in the City of Rome, Urban For. Urban Green. 37 (Jan. 2019) 13–23, https://doi.org/10.1016/j.ufug.2018.04.001.
[61] A. Screpanti and A. De Marco, "Corrosion on cultural heritage buildings in Italy: a role for ozone? Italian heritage buildings are at risk of corrosion caused by synergistic effects of O 3 and other pollutants," Environ. Pollut., vol. 157, pp. 1513–1520, doi: 10.1016/j.envpol.2008.09.046.
[62] M.S. Beldean-Galea, et al., Evaluation of indoor air pollutants in 100 retrofit residential buildings from Romania during cold season, J. Clean. Prod. (Sep. 2020), 124098, https://doi.org/10.1016/j.jclepro.2020.124098.
[63] D. de la Fuente, J.M. Vega, F. Viejo, I. Díaz, M. Morcillo, City scale assessment model for air pollution effects on the cultural heritage, Atmos. Environ. 45 (6) (Feb. 2011) 1242–1250, https://doi.org/10.1016/j.atmosenv.2010.12.011.
[64] J.L. Ramírez-Reyes, J. Uruchurtu-Chavarín, J. Genescá, R. Longoria-Ramírez, Evaluation of atmospheric corrosion in Orizaba, Mexico, Atmósfera 25 (4) (2012) 397–406.
[65] H.D. Kambezidis, G. Kalliampakos, Mapping atmospheric corrosion on modern materials in the greater Athens area, Water, Air, Soil Pollut. 224 (3) (2013), https://doi.org/10.1007/s11270-013-1463-y.
[66] F. Karaca, Mapping the corrosion impact of air pollution on the historical peninsula of Istanbul, J. Cult. Herit. 14 (2) (Mar. 2013) 129–137, https://doi.org/10.1016/j.culher.2012.04.011.
[67] A. De Marco, A. Screpanti, M. Mircea, A. Piersanti, C. Proietti, M.F. Fornasier, High resolution estimates of the corrosion risk for cultural heritage in Italy, Environ. Pollut. 226 (2017) 260–267, https://doi.org/10.1016/j.envpol.2017.03.066.
[68] F. Di Turo, et al., Impacts of air pollution on cultural heritage corrosion at European level: what has been achieved and what are the future scenarios, Environ. Pollut. 218 (2016) 586–594, https://doi.org/10.1016/j.envpol.2016.07.042.
[69] A.M. Navneet, Kaur Dhiman, Navneet Sidhu, Shekar Agnihotri, Role of nanomaterials in protecting building materials from degradation and deterioration, in: Biodegradation and Biodeterioration at the Nanoscale, 2021, https://doi.org/10.1016/B978-0-12-823970-4.00024-5.
[70] T. Utsev, T.M. Tiza, O. Mogbo, S.K. Singh, A. Chakravarti, N. Shaik, S.P. Singh, Application of nanomaterials in civil engineering, Mater. Today Proc. 62 (8) (2022) 5140–5146, https://doi.org/10.1016/j.matpr.2022.02.480.
[71] P. Ganguli, S. Chaudhuri, Proceedings Nanomaterials in antimicrobial paints and coatings to prevent biodegradation of man-made surfaces : a review, Mater. Today Proc. 45 (2021) 3769–3777, https://doi.org/10.1016/j.matpr.2021.01.275.
[72] I. Franco-castillo, L. Hierro, M. De Fuente, S.G. Mitchell, Review Perspectives for Antimicrobial Nanomaterials in Cultural Heritage Conservation, 2021, pp. 629–669, https://doi.org/10.1016/j.chempr.2021.01.006.